RP Current Trends in Engineering and Technology
Vol. 2, No. 1 (January – March 2023) pp. 13–22
e-ISSN: 2583-5491

RESEARCH PLATEAU PUBLISHERS

Cite this article: J. Singh, Parametric excitation of optical phonons in weakly-polar narrow band gap magnetized semiconductors, *RP Cur. Tr. Eng. Tech.* **2** (2023) 13–22.

Original Research Article

Parametric excitation of optical phonons in weakly-polar narrow band gap magnetized semiconductors

Jaivir Singh
Department of Physics, J.V.M.G.R.R. College, Charkhi Dadri - 127306, Haryana, India
*Corresponding author, E-mail: jaivir.bmu@gmail.com

ARTICLE HISTORY
Received: 12 Oct. 2022
Revised: 12 Jan. 2023
Accepted: 13 Jan. 2023
Published online: 15 Jan. 2023

KEYWORDS
Parametric excitation; optical phonons; narrow band gap semiconductors.

ABSTRACT
An analytical treatment based on the hydrodynamic model of plasmas is developed to study parametric amplification and oscillation of optical phonon modes in weakly polar narrow direct gap magnetized semiconductors. Second-order optical susceptibility arising due to nonlinear polarization and the basic operational characteristics of the parametric device, viz., threshold nature, power gain mechanisms and conversion efficiency, are obtained. The effects of doping, magnetic field and excitation intensity, on the above operational characteristics have been studied in detail. Numerical estimates are made for an n-InSb crystal at 5 K duly irradiated by a pulsed 10.6 μm CO_2 laser. The nature of the variation of the power gain with respect to the pump intensity and that of the threshold condition for parametric oscillation with respect to signal reflectance and sample length are found to be in good qualitative agreement with the experimental observations in electro-optic materials such as $Ba_2NaNb_5O_{15}$ and $LiNbO_3$. The analysis suggests the possibility of observing super-fluorescent parametric emission and oscillation in moderately doped n-InSb crystal under off-resonant nanosecond pulsed not-too-high power laser irradiation, the crystal being immersed in a large magnetic field.

1. Introduction

Understanding and controlling the interaction between light and matter are of fundamental importance to a wide range of applications in science and technology. More than a century ago, puzzles over blackbody radiation and atomic line spectra led to the birth of quantum mechanics and there have been innumerable developments since, not least the laser. Since the invention of the laser, a major area of optoelectronics has been devoted to the development of optical devices capable of providing tunable coherent radiation through the electromagnetic spectrum. Laser light can be used to control matter as in optical tweezers to manipulate cells [1]. Surface plasmon polaritons are also being developed as bio-molecule sensors [2]. On the other hand, optical bistable studies explore possible ways to control light with light [3].

Parametric amplification and oscillation in the radio frequency and microwave range [4] were demonstrated before the laser was invented. The same process was expected in the optical region and was actually demonstrated in 1965 by Giordmaine and Miller [5]. It has since become an important effect because it allows the construction of widely tunable coherent infrared sources through the controllable decomposition of the pump frequency. Optical parametric amplifiers and oscillators (OPA/OPO) provide a convenient method of generating tunable radiation over broad spectral ranges and one of their very useful characteristics is the low noise level. Further backward OPO was proposed in 1966 by Harris [6], which sparked many efforts to implement it through backward parametric fluorescence [7] and backward difference frequency generation [8].

In optical parametric amplification, a weak signal is made to interact with a strong, higher frequency pump and both the generated difference frequency (known as the idler) and the original signal are amplified. If the idler and the amplified signal are passed through the mixing crystal again, with the proper phase, both are again amplified. In addition, if either one is passed through the crystal again with the proper phase; the result is still a gain in both. Thus, the amplifier can be made into an oscillator by adding the proper feedback (i.e. a resonator) to both the signal and the idler, or by resonating only one. If the gain per path is larger than the loss per path, the signal can build up out of the noise, and the system will oscillate. It is well known that by resonating only the signal or idler in an optical parametric oscillator, both output power stability and the tuning range are improved [9]. Recently major enhancements in the overall performance of continuous wave single resonant parametric oscillator (SRPO) through finite output coupling of the resonant wave [10] and gain width and rise time studies of pulsed unstable OPOs [11] have been reported. Various effective methods of generating eye safe radiations [12] and light in the yellow [13] and blue [14] spectral region based on OPO characteristics are also being developed. The developments in the field of parametric amplifiers and oscillators and their usage are restricted to a large extent due to the inherent material limitations, viz., low optical damage threshold, inadequate birefringence and optical transparency range.

The advent of new nonlinear materials with high-optical-damage threshold, wide optical transparency range and laser

pump sources of improved spectral and spatial coherence has created new vistas for generating widely tunable optical coherent radiation using OPA/OPO. Amongst the various nonlinear materials, the semiconductor crystals (especially III-V semiconductors) are substantially transparent for photon energies much less than the band-gap energies [15] and undergo optical damage at considerably large excitation intensities [16]. In addition, semiconductors have added advantages over other materials in terms of compactness, control over the material relaxation times, observed large nonlinearities in optical properties under near resonant laser irradiation and sophisticated fabrication technology [17]. Furthermore, a variety of interesting nonlinear optical processes have been observed due to the excess free concentration in doped semiconductors [18].

In the recent past, parametric amplification and oscillation over an infrared spectral regime have been studied theoretically as well as experimentally in urea, liquid crystals, KTP, $MgO:LiNbO_3$ and $SrTiO_3$ etc [19-22]. Dubey and Ghosh [23] studied parametric oscillation of polaron modes in magnetized semiconductor plasmas. To the author's knowledge, so far, no systematic study has yet been made to critically examine the possibility of developing OPA/OPO using weakly polar narrow direct-gap magnetized semiconductors like GaAs, GaSb, InAs, InSb etc. with optical phonons acting as the idler wave. Such crystal classes are usually partially ionic and, therefore, the piezoelectric scattering is often overshadowed by optical phonon scattering mechanisms [24]. The study of the propagation characteristics of coherent optical phonon wave is of substantial importance in the investigation of the fundamental properties of solids. The study of longitudinal optical phonon-laser interactions in semiconductors has been one of the most active fields of research due to its vast potentiality in spectroscopy and high speed optoelectronic devices.

Keeping in view the possible impact of parametric interactions involving an optical phonon mode, we present here an analytical study of OPA/OPO using the n-type doped III-V crystals immersed in a large static magnetic field following the hydrodynamic model for the semiconductor-plasma. The only nonlinearity that is taken into account in the present analysis has its origin in the nonlinear coupling between the generated density perturbations at both signal and idler frequencies and the pump electric field.

2. Theoretical formulations

The theory of nonlinear interaction has been discussed by many authors both from classical and quantum mechanical view points. If there are many photons in the radiation field it can be properly described by classical waves. In the treatment of coupled wave problems, the classical description is even more appropriate since then the decay or amplification of the waves depends on the relative phases among them, whereas in the quantum mechanical description, if the number of quanta is prescribed, the phases will be undetermined as required by uncertainty principle. Thus, here, we consider the hydrodynamic model of homogeneous semiconductor-plasma. It restricts our analysis to be valid in the limit $kl \ll 1$ (k is the wave number and l is the carrier mean free path).

In order to study OPA and OPO due to excitation of optical phonon mode in magnetized semiconductor plasmas, we consider the crystal sample to be irradiated by a pump wave $(\omega_0, \vec{k}_0)$ under thermal equilibrium conditions. The static magnetic field $\vec{B}_s$ is taken to be parallel to the z-axis, normal to the propagation vectors $\vec{k}_0$, $-\vec{k}_s$ and $\vec{k}_{op}$ (all parallel to the x-axis) of three interacting waves, viz, pump $(\omega_0, \vec{k}_0)$, signal $(\omega_s, -\vec{k}_s)$ and idler (optical phonons $\omega_{op}, \vec{k}_{op}$), respectively. The momentum and energy exchange between these waves can be described by phase-matching conditions: $\hbar\vec{k}_0 = -\hbar\vec{k}_s + \hbar\vec{k}_{op}$ and $\hbar\omega_0 = \hbar\omega_s + \hbar\omega_{op}$ which yield $\omega_s = \omega_0 - \omega_{op}$ and $\vec{k}_{op} = 2\vec{k}_s = \vec{k}$ (since $|\vec{k}_0| \cong |\vec{k}_s|$). The present analysis is based upon the coupled mode approach. The backward Stoke's mode $(\omega_s, -\vec{k}_s)$ originates from the coupling of the pump wave with density perturbations at an optical phonon frequency ω_{op} in the crystal. The coupling of the pump and the Stoke's wave generates a strong electrostatic field (space-charge field) oscillating at frequency ω_{op}. This generated optical phonon field possesses both transverse and longitudinal components. In the weakly polar semiconductors (viz., GaAs, InSb), the longitudinal optical (LO) phonons are accompanied by a longitudinal electric field while transverse optical (TO) phonons are associated with the transverse electrostatic field. The intensities of LO and TO phonons scattering become unrelated for finite $\vec{k}$ because they are determined by two independent parameters, viz., the electro-optical effect and the deformation potential Raman tensor, respectively [25]. It is well known that the polarization associated with the longitudinal vibration is much larger than the transverse component in III-V crystals like InSb, GaAs, etc. with zinc-blend structures [26]. Consequently, we neglect the transverse electric field and treat ω_{op} as the longitudinal optical phonon frequency.

The passive medium is taken as a diatomic crystal with the two atoms in the molecule vibrating in opposite directions. This diatomic molecule is characterized by its position and normal vibration coordinates $u_{\pm}(x,t)$. In the presence of electromagnetic radiation, the equation of motion for a single oscillator under one dimensional (1-d) configuration can be given as [27]

$$\frac{\partial^2 s(x,t)}{\partial t^2} + \omega_{opo}^2 s(x,t) + 2\Gamma_{op}\frac{\partial s(x,t)}{\partial t} = \frac{q_s}{M}E_{op} \qquad (1a)$$

where $s(=u_+ + u_-)$ is the relative displacements of positive and negative ions, respectively. In Eq. (1a), ω_{opo} is the optical phonon frequency at $\vec{k}_{op} = 0$. Γ_{op} takes into account the phonon decay and is introduced phenomenologically as a constant parameter. The value of Γ_{op} is taken to be $10^{-2}\omega_{opo}$ [28, 29]. q_s is the Szigeti effective charge and defined as [30]

$$q_s = \omega_{opo}\left[\frac{M}{N}\varepsilon_0\left(\frac{1}{\varepsilon_s} - \frac{1}{\varepsilon_\infty}\right)\right]^{1/2}, \qquad (1b)$$

where, M and $N(=a_l^3)$ are the reduced mass of the diatomic molecule and number of unit cell per unit volume, respectively; a_l is the lattice constant of the crystal. ε_0 is the permittivity of free space, while ε_s and ε_∞ are static and high

frequency dielectric constant of the crystal, respectively. E_{op} is the macroscopic internal electrostatic field oscillating at the optical phonon frequency ω_{op}. It is convenient to write the relative displacement in terms of new parameter *w* defined as [31]: $w=(NM)^{1/2}s$. Accordingly, equation (1a) can be expressed as:

$$\frac{\partial^2 w(x,t)}{\partial t^2}+\omega_{opo}^2 w(x,t)+2\Gamma_{op}\frac{\partial w(x,t)}{\partial t}=\left(\frac{q}{M}\right)^{1/2}q_s E_{op}. \tag{1c}$$

The two ions have opposite charges; therefore there will be a net oscillation dipole moment in the crystal and, hence, induces a polarization ($P=q_s w$). The induced longitudinal phonon electrostatic field (E_{op}), arising due to the induced polarization can be calculated by using Poission's equation. Consequently E_{op} can be expressed in terms of the polarization as:

$$\frac{\partial E_{op}}{\partial x}=-\frac{n_{op}e}{\varepsilon}-\frac{Nq_s}{\varepsilon}\left(\frac{\partial w}{\partial x}\right) \tag{2}$$

where $\varepsilon=\varepsilon_0\varepsilon_\infty$; n_{op} is the carrier density perturbation oscillating at the optical phonon frequency and $-e$ is electronic charge. At the entrance window $x=0$, the density perturbation n_{op} may be taken to be small enough such that $n_{op}(e/E)$ can be neglected in equation in Eq. (2) and we obtain

$$E_{op}=\left|\frac{Nq_s}{k\varepsilon}\left(\frac{\partial w}{\partial x}\right)\right| \tag{3}$$

where we have taken $\left|\vec{k}_{op}\right|=k$ (say). E_{op} can be estimated approximately in the weakly polar III-V semiconductor crystals from the knowledge of strain $(\partial w/\partial x)$. Assuming $(\partial w/\partial x)=10^6$ [32, 33], we get $E_{op}(0)=2.15\times10^5\,\mathrm{Vm^{-1}}$ in n-InSb crystal with $M=2.7\times10^{29}\,\mathrm{kg}$, $N=(a_l^3)=3.7\times10^{27}\,\mathrm{m^{-3}}$, $k=1.86\times10^6\,\mathrm{m^{-1}}$, $\varepsilon_s=17.54$, $\varepsilon_\infty=15.68$, and $q_s=1.2\times10^{-20}\,\mathrm{C}$ (obtained by using Eq. 1(b)).

The other basic equations governing the three-wave interactions are:

$$n_0\frac{\partial v_1}{\partial x}+v_0\frac{\partial n_1}{\partial x}+\frac{\partial n_1}{\partial t}=0 \tag{4}$$

$$\frac{\partial \vec{v}_0}{\partial t}+\nu\vec{v}_0=-\frac{e}{m}(\vec{E}_0+\vec{v}_0\times\vec{B}_s) \tag{5}$$

$$\frac{\partial \vec{v}_1}{\partial t}+\nu\vec{v}_1+(\vec{\nabla}.\vec{v}_1)\vec{v}_0=-\frac{e}{m}(\vec{E}_1+\vec{v}_1\times\vec{B}_s) \tag{6}$$

Eq. (4) represents the continuity equation with n_0 being the dc electron concentration. Eqs. (5) and (6) are the zeroth and first order electron momentum transfer equations, $\vec{v}_0$ and $\vec{v}_1$ being the zeroth and first order oscillatory electron velocities, respectively. Also ν and *m* are the electron-electron collision frequency and electron effective mass respectively.

In order to obtain the coupled mode equation for the optical phonon flux, we consider the density perturbations n_{op} and n_s have phase factors like $\exp[i(k_{op}x-\omega_{op}t)]$ and $\exp[i(-k_s x-\omega_s t)]$, respectively. These density perturbations can be obtained by using Eq. (4) as follows:

$$n_{op}=\frac{k}{\omega_{op}}(n_s v_0+n_0 v_{op}) \tag{7a}$$

and

$$n_s=\frac{k}{\omega_s}(n_{op}v_0^*+n_0 v_s). \tag{7b}$$

Here, $v_{op}=\dfrac{-(e/m)(\nu-i\omega_{op})}{\omega_c^2+(\nu-i\omega_{op})^2}E_{op}$

and $v_s=\dfrac{-(e/m)(\nu-i\omega_s)}{\omega_c^2+(\nu-i\omega_s)^2}E_s$,

with $n_1=n_{op}+n_s$ and $v_1=v_{op}+v_s$ and $\omega_c[=-e/m)B_s]$ is the cyclotron frequency. Substitution of values of *u* and n_{op} from Eqs. (1a) and (7a), in Eq. (2) and simple mathematical simplification yield

$$\left(1+\frac{Nq_s^2}{\varepsilon M\omega_{pp}^2}\right)\frac{\partial E_{op}}{\partial x}=\frac{ek}{\varepsilon\omega_{op}}(n_s v_0+n_0 v_{op}), \tag{8}$$

where $\omega_{pp}=(\omega_{opo}^2-\omega_{op}^2-2i\Gamma_{op}\omega_{op})^{1/2}$.

It is evident from Eq. (8) that the coupling of the perturbed electron density and oscillatory electron fluid velocity act as a disturbed source that can feed energy to the induced optical phonon field (E_{op}) leading to the amplification of this field with a large gain coefficient. Eq. (8) can also be expressed in terms of the coupled electric fields. Using Eqs. (3-5) and (8), the induced longitudinal optical phonon flux can be calculated as

$$\frac{\partial E_{op}}{\partial x}+\alpha_{op}E_{op}=i\beta_1 E_0(x)E_s(x). \tag{9a}$$

Here $\alpha_{op}E_{op}$ is introduced phenomenologically to take into account the absorption processes in the crystal; α_{op} being the absorption coefficient in the off-resonant regime. β_1 is treated as the coupling parameter which can be obtained from the above formulations as

$$\beta_1=\frac{-iek^2}{m\omega_0\omega_{op}\delta_0}\left[1+\frac{Nq_s^2}{\varepsilon M\omega_{pp}^2}+\frac{i\omega_p^2(\nu-i\omega_{op})}{\omega_{op}[(\nu-i\omega_{op})^2+\omega_c^2]}\right]^{-1} \tag{9b}$$

where, $\delta_0=1-(\omega_c/\omega_0)^2$. We have also considered both ω_0 and ω_s to be much larger than ν. $\omega_p[=(n_0e^2/m\varepsilon)]^{1/2}$ is the electron-plasma frequency. In order to obtain the steady state coupled mode equations for the pump and the Stoke's

waves, we employ Maxwell's equations in the presence of a finite induced nonlinear polarization P_{nl} arising due to the nonlinear current density given by

$$\nabla^2 \vec{E} = \frac{1}{c_1^2}\frac{\partial^2 \vec{E}}{\partial t^2} - \mu_0 \frac{\partial^2 \vec{P}_{nl}}{\partial t^2}. \tag{10}$$

where c_1 is the velocity of light in the crystal. $\vec{P}_{nl} = \int \vec{J} dt$, where $\vec{J} = \vec{J}_0 + \vec{J}_1$ represents the total induced current density in the crystal and comprises the zeroth- order ($\vec{J}_0$) as well as the perturbed components oscillating at the Stoke's frequency $\vec{J}_1(\omega_s)$. We have restricted ourselves only to the infrared transparency region where photon energies are less than the crystal band gap energies. Thus, one can neglect the effect of the induced transition dipole moment in the crystal. The complex optical susceptibility $\chi = \chi_r + i\chi_i$ can be obtained from

$$P_{nl} = \varepsilon_0 \chi E = \varepsilon_0 [\chi^{(1)} + \chi^{(2)} E] E \tag{11a}$$

where

$$\vec{P}_{nl} = \int \vec{J} dt = -\int (n_0 e v_s + n_{op} e v_0^*) dt. \tag{11b}$$

In Eq. (11a), we have truncated the expression up to the second-order nonlinear optical susceptibility ($\chi^{(2)}$) since the origin of the three-wave parametric interactions lies in $\chi^{(2)}$ of the medium. Using Eqs. (10)-(11) and employing the slowly varying envelope approximation (SVEA), we obtain in the 1-d configuration

$$\frac{\partial E_0}{\partial x} + \alpha_0 E_0 = i\beta_{20} E_{op}(x) E_s^*(x) \tag{12a}$$

and

$$\frac{\partial E_s}{\partial x} + \alpha_s E_s = i\beta_{2s} E_{op}(x) E_0^*(x). \tag{12b}$$

Eqs. (12) represent coupling of the pump and the backward scattered Stoke's wave via the optical phonon vibrations in the medium. α_0 and α_s are the inherent backward absorption coefficient at frequency ω_0 and ω_s defined as $\alpha_{0,s} = (\omega_{0,s}/\eta c)\chi_i^1$; η being the crystal background refractive index and $k_{0,s} = (\eta\omega_{0,s}/c)$. One can find $\chi_i^{(1)}$ in the presence of a strong magneto static field B_s by using Eqs. (6) and (11) as

$$\chi_i^{(1)} = \varepsilon_\infty \frac{\omega_p^2 \nu}{\omega_s^3} \frac{\delta_s}{\delta_s^2 + (\nu^2/\omega_s^2)} \tag{13}$$

where $\delta_s = 1 - (\omega_c/\omega_s)^2$. $\beta_{20,s}$ as introduced in Eq. (12) is the coupling parameter which is defined as

$$\beta_{20,s} = \frac{\omega_{0,s}}{2\eta c}\chi^{(2)} \tag{14}$$

with $\chi^{(2)}$ being the second-order optical susceptibility of the crystal at finite magnetic field.

Following Aghamkar and Sen [34] and using Eqs. (1-6) and (11), $\chi^{(2)}$ can be obtained as

$$\chi^{(2)} = \frac{-iekNq_s^2}{\varepsilon_0 mM} \frac{\omega_p^2}{\omega_0\omega_s\delta_0\delta_s\omega_{pp}^2\Omega^2}, \tag{15}$$

where $\Omega^2 = (\omega_p^2/\delta_s) - \omega_{op}^2 + i\nu\omega_{op}$.

We now address ourselves to the analytical study of operational characteristics of the optical parametric amplifiers and oscillator. We employ Eqs. (9) and (12b) and solve them assumed solution of the forms [16]

$$E_{op}(x) = C_1 \exp(\gamma x) \tag{16a}$$

and

$$E_s(x) = C_2 \exp(\gamma x); \tag{16b}$$

C_1 and C_2 are the arbitrary constants and γ is the gain coefficient. One may recall that the parametric interactions yield identical gain coefficients for both the signal and idler waves. The gain coefficient can be determined by using Eqs. (9) and (12b) through Eq. (16). Simplification yield

$$\begin{vmatrix} \gamma + \alpha_{op} & i\beta_1 E_0(0) \\ i\beta_2 E_0^*(0) & \gamma + \alpha_s \end{vmatrix} \begin{vmatrix} E_{op} \\ E_s \end{vmatrix} = 0. \tag{17}$$

We obtain

$$\gamma_\pm = \frac{-\alpha_s \pm \gamma_0}{2} \tag{18}$$

with $\gamma_0 = [\alpha_-^2 - (8\beta_1\beta_2/\eta\varepsilon_0 c)I_p]^{1/2}$ and pump intensity $I_p = (1/2)\eta\varepsilon_0 c|E_0|^2$. For simplicity, we consider $\alpha_\pm = \alpha_{op} + \alpha_s$. Also we have assumed $\beta_{20} = \beta_{2s} = \beta_2$ for $\omega_0 \sim \omega_s \gg \omega_{op}$.

Consequently, we get form Eq. (16)

$$E_{op}(x) = \exp\left(-\frac{\alpha_+ x}{2}\right)\left[C_{1+}\exp\left(\frac{\gamma_0 x}{2}\right) + C_{1-}\exp\left(\frac{-\gamma_0 x}{2}\right)\right] \tag{19a}$$

and

$$E_s(x) = \exp\left(-\frac{\alpha_+ x}{2}\right)\left[C_{2+}\exp\left(\frac{\gamma_0 x}{2}\right) + C_{2-}\exp\left(\frac{-\gamma_0 x}{2}\right)\right]. \tag{19b}$$

In order to study the parametric amplification as well as oscillations in the direct-gap weakly polar semiconductor crystal, we consider $E_{op}(0)$ to be finite due to the lattice vibrations. Also $E_s(0)$ is non-vanishing due to finiteness of the spontaneous noise field. These considerations enable one to determine the signal and the idler fields at the exit window

$x = L$ with L being the sample length. Using the above boundary conditions, we obtain

$$C_{1+} = \frac{1}{2\gamma_0}\left[(\gamma_0 \mp \alpha_-)E_{op}(0) \pm 2i\beta_1 E_0(0)E_s(0)\right] \quad (20a)$$

and

$$C_{2+} = \frac{1}{2\gamma_0}\left[(\gamma_0 \pm \alpha_-)E_s(0) \pm 2i\beta_2 E_{op}(0)E_0^*(0)\right]. \quad (20b)$$

We also obtain

$$E_{op}(L) = \exp\left(\frac{-\alpha_+ L}{2}\right)\left[\left\{\cosh(\gamma_0 L) - \left(\frac{\alpha_-}{\gamma_0}\right)\sinh(\gamma_0 L)\right\}E_{op}(0) + \left(\frac{2i\beta_1}{\gamma_0}\right)E_0(0)E_s(0)\sinh(\gamma_0 L)\right] \quad (21a)$$

and

$$E_s(L) = \exp\left(\frac{-\alpha_+ L}{2}\right)\left[\left\{\cosh(\gamma_0 L) - \left(\frac{\alpha_-}{\gamma_0}\right)\sinh(\gamma_0 L)\right\}E_s(0) + \left(\frac{2i\beta_1}{\gamma_0}\right)E_{op}(0)E_0^*(0)\sinh(\gamma_0 L)\right]. \quad (21b)$$

Eqs. (21) describe the output signal and idler waves in a parametric amplifier. The above basic formulations can be employed to study the device characteristics like threshold behavior, gain spectra and conversion efficiency of the OPA/OPO.

3. Parametric amplifier

3.1 Threshold condition

The threshold condition for the onset of parametric amplification for the case of a semiconductor can be studied by using Eq. (18). The threshold value of the pump intensity I_{pth} required for the onset of the parametric amplification in the presence of an externally applied magnetic field is obtainable from Eq. (18) by setting $\gamma_\pm = 0$. This yields

$$(I_{pth})_{PA} = \frac{\eta\varepsilon_0 c}{4}\left|\frac{\alpha_{op}\alpha_s}{\mathrm{Re}(\beta_1\beta_2)}\right| \quad (22)$$

where 'Re' denotes real part of $\beta_1\beta_2$. Eq. (22) will be used to study the effects of the excess carrier concentration n_0 (through ω_p) and the externally applied magnetic field B_s (through ω_c) on the threshold condition of the parametric amplifier.

3.2 Power gain of parametric amplifier

With the assumption that the pump intensity is well above threshold, the single-pass power gain $g_{i(s)}$ of the idler (signal) wave can be expressed through the relation [16]

$$g_{i(s)} = \left|\frac{E_{op(s)}(L)}{E_{op(s)}(0)}\right| - 1. \quad (23a)$$

Eq. (23a) manifests amplification of the generated modes (E_{op} or E_s). Keeping in view that input noises value of the Stoke's field is negligibly small (viz, $E_s(0) = 10^{-6}E_0(0)$) [35], we have restricted ourselves to the study of amplification of the optical phonon flux in the high gain regime (i.e., $\mathrm{Re}(\beta_1\beta_2)I_p \gg \alpha_+^2$). Consequently, we obtain the power gain factor for the idler wave as

$$g_i(L) = \frac{1}{4}\left|\exp\left\{\frac{2I_p\,\mathrm{Re}(\beta_1\beta_2)}{\eta\varepsilon_0 c}\right\}^{1/2} L\right|. \quad (23b)$$

This equation shows that energy can be transferred from the pump to the idler and is useful in understanding the phenomena of super-fluorescent parametric emission of the idler wave [16].

4. Single resonant parametric oscillator (SRPO)

In order to study basic operational characteristic of the SRPO, we consider that a parametric amplifier satisfying Eq. (21) is placed inside an optical cavity such that we can have feedback of Stoke's field. If the parametric amplified power gain is sufficiently high, a parametric oscillator can be constructed [16]. The consideration of feedback mechanism makes it possible for the parametric gain to overcome the losses and subsequently parametric oscillations occur.

4.1 Threshold condition

Here, we have made an attempt to establish the weakly polar III-V semiconductor crystals as the class of materials suitable for the development of SRPO. The SRPO has many advantages over the double resonant parametric oscillator (DRPO) except that it requires large threshold pump intensity. Therefore, we have chosen SRPO for the present study. The optical cavity configuration for SRPO has been chosen such that the second mirror located at exit window of the cavity is strongly reflective at the Stoke's wave frequency ω_s whereas, for the pump and optical phonon frequencies ω_0 and ω_{op}, both the mirrors are nearly transparent. We have taken R_s as the Stoke's field reflectivity parameter of the second mirror. In this analysis, we have neglected the phase shifts in phonon and Stoke's field due to traversal and reflection in the cavity [36]. For simplicity it is also assumed that the cavity length is equal to the crystal length L. In order to reduce the threshold value of the pump intensity and to enhance the power gain of the optical phonon modes well above the threshold, we have employed the round-trip mechanism [16]. Under such circumstances, the threshold condition can be given by

$$R_s\left|E_s(L)\right| = \left|E_s(0)\right|. \quad (24)$$

Physically, Eq. (24) signifies that the Stoke's field neither amplifies nor decays during one round-trip. While considering the attenuation loss due to absorption and scattering in the cavity as well as the mirror transmission loss, the total loss in the cavity may be expressed as [37]

$$\alpha_{T+} = \alpha_{\pm} - \frac{1}{L}(\ln R_s)\,. \tag{25}$$

Using Eqs. (21b), (24) and (25), we obtain

$$\left|\exp\left(\frac{-\alpha_{T+}L}{2}\right)\mathrm{Re}(\beta_2)R_s E_{op}(0)\sinh(\gamma_0' L)\right| = \left|\gamma_0'\frac{E_s(0)}{E_0(0)}\right| \tag{26}$$

$$\text{with } \gamma_0' = \left[4\alpha_{T-}^2 + 8\,\mathrm{Re}(\beta_1\beta_2)\left(\frac{I_p}{\eta\varepsilon_0 c}\right)\right]^{1/2};\ E_s(0) \ll E_0(0)\,.$$

Eq. (26) can be differentiated with respect to γ_0' to get the threshold pump intensity for SRPO as

$$(I_{pth})_{SRPO} = \left|\frac{\eta\varepsilon_0 c}{8\,\mathrm{Re}(\beta_1\beta_2)}\left[\frac{1}{L^2}\left\{\cosh^{-1}\left(\frac{1}{Q}\right)\right\}^2 - 4\alpha_{T-}^2\right]\right|, \tag{27}$$

$$\text{where } Q = \exp\left(\frac{-\alpha_{T+}L}{2}\right)LR_s E_{op}(0)\,\mathrm{Re}(\beta_2)\frac{E_0(0)}{E_s(0)}\,.$$

4.2 Conversion efficiency of parametric oscillator

In this subsection, we have addressed ourselves to the calculation of the conversion efficiency in weakly polar III-V semiconductor crystals. The conversion efficiency $\eta_{i(s)}$ is defined as the ratio of the idler (signal) output energy to the incident pump energy. In order to estimate the conversion efficiency of the parametric oscillator, relation between the idler (signal) power to constant signal (idler) power must be known [16, 37]. In the present article, this relation can be derived from the set of coupled mode Eqs. (9) and (12a). In doing so, we have assumed the signal field (Stoke's mode) as constant during single round-trip. Solving Eq. (9) and (12a) and obtained simplified solution of the idler mode as

$$E_{op}(L) = \exp(-\alpha_{T+}L)\left[\left\{\cosh(\gamma_2 L) - \left(\frac{\alpha_{T-}}{\gamma_1}\right)\sinh(\gamma_2 L)\right\}E_{op}(0) + \left(\frac{2i\beta_1}{\gamma_1}\right)E_0(0)E_s(0)\sinh(\gamma_2 L)\right], \tag{28}$$

$$\text{where } \gamma_1 = -\alpha_{T-} + \gamma_2,\ \gamma_2 = \left[\alpha_{T-}^2 + \mathrm{Re}(\beta_1\beta_2)|E_s|^2\right]^{1/2}.$$

Using Eq. (28) and the definition of η_i as given above, we can have

$$\eta_i = \frac{|E_{op}(L)|^2}{|E_0(0)|^2}\,. \tag{29}$$

Eq. (29) can be employed to study the role of magnetic field as well as doping on the conversion efficiency under slightly off-resonant laser excitation with pump intensity well above the threshold.

5. Results and discussion

In this section, we have made a detailed numerical analysis of the operational characteristics of the OPA/OPO using III-V semiconductors in the presence of a static magnetic field. Special emphasis is laid on the dependence of operational characteristics on the system parameters like doping concentration n_0, applied magnetic field B_s and pump intensity I_p. The material system selected for the numerical analysis is n-InSb duly irradiated by a pulsed 10.6 μm CO_2 laser with pulse duration of 10 nanosecond. The other relevant material parameters are [23, 28]: $m = 0.014m_0$ (m_0 being the free electron mass), $k = 1.86\times10^6\,\mathrm{m}^{-1}$, $\nu = 10^{11}\,\mathrm{s}^{-1}$ (electron-electron collision frequency), $\alpha_{op} = 100\,\mathrm{m}^{-1}$ [15] and the sample length $L \geq 400\,\mu\mathrm{m}$. The pump frequency ω_0 (corresponding to 10.6 μm wavelength of the CO_2 laser) is $1.78\times10^{14}\,\mathrm{s}^{-1}$. The longitudinal component of the optical phonon frequency ω_{op} can be defined as $\omega_{op} = k_B\theta_D/\hbar$, k_B and θ_D being Boltzmann's constant and Debye temperature of the lattice, respectively. With $\theta_D = 278\mathrm{K}$ [38] for n- InSb crystal, we get $\omega_{op} = 3.64\times10^{13}\,\mathrm{s}^{-1}$.

5.1 Threshold and power gain of OPA

Making use of the material parameters for InSb crystal as given above in Eq. (22), the threshold nature of the parametric amplification has been studied. In weakly polar semiconductors, the longitudinal optical phonon emission rate depends upon the excess carrier energy as well as its density. This emission rate is constant at low n_0 and decreases sharply with $n_0 > 10^{22}\,\mathrm{m}^{-3}$ ($\omega_p > 1.7\times10^{14}\,\mathrm{s}^{-1}$) while studying operational characteristics of OPA/SRPO.

Fig. 1 represent the analytical dependence of the threshold intensity $(I_{pth})_{PA}$ on the applied magnetic field (in terms of ω_c). It can be seen that $(I_{pth})_{PA}$ decreases sharply and achieves a minimum value at $\omega_c = 0.60\times10^{14}\,\mathrm{s}^{-1}$ ($B_s = 4.8\,\mathrm{T}$). This dip may be attributed to the fact that at $B_s = 4.8\,\mathrm{T}$ resonance between ω_c and $2\omega_{op}$ occurs. For $0.7\times10^{14}\,\mathrm{s}^{-1} < \omega_c < 1.24\times10^{14}\,\mathrm{s}^{-1}$, $(I_{pth})_{PA}$ is independent of magnetic field. Further increase in the value of magnetic field causes increase in $(I_{pth})_{PA}$. Around $\omega_c = 1.38\times10^{14}\,\mathrm{s}^{-1}$ ($B_s = 11\,\mathrm{T}$), we have $\omega_c \sim \omega_s < \omega_0$, and the threshold intensity exhibits a peak. Still higher magnetic field causes sharp fall in the threshold value of the pump intensity required for the onset of parametric amplification. For $\omega_c \leq \omega_s \leq \omega_0$, Fig. 1 exhibits a sharp fall in the threshold intensity and the minimum threshold is obtained for $\omega_c \sim \omega_0$. In moderately doped n-type InSb crystal, such lowering of threshold intensity by applying a magnetic field $B_s = 14.2\,\mathrm{T}$ makes this crystal a potential candidate material for parametric amplification studies. With

further increase in magnetic field (resulting in $\omega_c > \omega_0$), the departure from the resonance causes increase in $(I_{pth})_{PA}$ and that finally saturates at a considerably large value. Hence it can be concluded that resonant enhancement of the threshold input intensity for the onset of OPA occurs when the electron cyclotron frequency is equal to signal frequency, whereas resonant decrement takes place when cyclotron frequency approaches towards pump wave frequency.

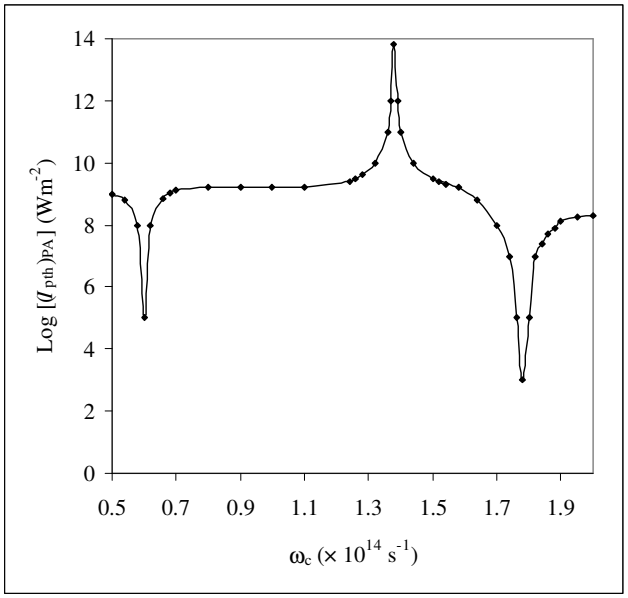

Figure 1: Variation of the threshold intensity $(I_{pth})_{PA}$ of the parametric amplifier with magnetic field B_s (in terms of ω_c). Here $n_0 = 2\times10^{21}\text{m}^{-3}$ ($\omega_p = 5.4\times10^{12}\text{s}^{-1}$).

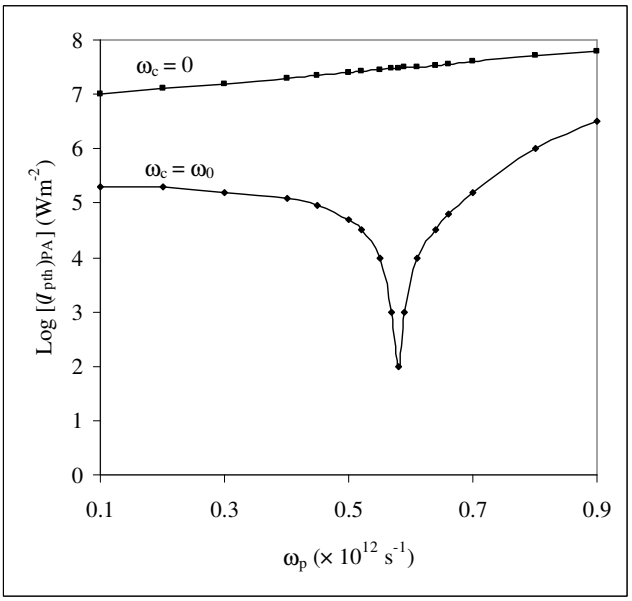

Figure 2: Variation of threshold pump intensity $(I_{pth})_{PA}$ with carrier concentration n_0 (in terms of ω_p) in the absence ($\omega_c = 0$) and presence ($\omega_c = \omega_0$) of magnetic field.

Fig. 2 is plot of the threshold intensity (both in the presence and absence of a magnetic field) as a function of the doping concentration (in terms of ω_p). In the absence of magnetic field ($\omega_c = 0$), $(I_{pth})_{PA}$ increases linearly with increasing doping concentration. On the other hand, in the presence of magnetic field ($\omega_c = \omega_0$), $(I_{pth})_{PA}$ remains almost constant initially and shows a dip at $\omega_p = 5.8\times10^{14}\text{s}^{-1}$ ($\omega_p^2 \sim \delta_0\omega_{op}^2$). Thereafter the threshold intensity varies as a function of doping concentration. It is clear from Figs. 1 and 2 that $(I_{pth})_{PA}$ can be reduced from 10^6 to 10^3 Wm^{-2} in n-InSb by the proper selection of magnetic field magnitude and doping concentration.

In order to study the spectral behaviour of super-fluorescent parametric amplifier through the power gain parameters $g_{i(s)}(L)$, we have used the Eq. (23b). Here, we have confined ourselves to the study of power gain of optical phonon in n-InSb. The parametric gain of the signal in this crystal has been studied recently by one of the present authors [39]. The efficient super-fluorescent parametric operation can be achieved if the power gain is extremely high, such that the power gain factor $g_i(L)$ represented by Eq. (23b) is found to be as large as 10^{16} [16]. In order to achieve this, we have chosen $I_p \sim 10^{11}\text{Wm}^{-2}$ and $L = 400\,\mu\text{m}$.

It appears worth discussing that at such high excitation intensities of the 10.6 μm pulsed CO_2 laser, a large free carrier density may be created in InSb crystal, via two-photon absorption mechanism. Such carrier generation depends critically on the proximity of the crystal band gap energy $\hbar\omega_g$ to the two-photon energy $\hbar\omega_0$. As is well known, the possibility of the two-photon absorption induced free carrier generation can be minimized by increasing the crystal band gap. This is achieved successfully by choosing a low crystal temperature. Accordingly, we have selected the crystal temperature around 5 K when $\hbar\omega_g = 0.2368\,\text{eV}$ for InSb [40]. Consequently the two-photon absorption can be eliminated and the three-photon absorption probability being obviously small with $\hbar\omega_g \ll 3\hbar\omega_0$, and, therefore, one can neglect the photo generation of free carriers. It may be also noted that the parametric gain factor can be increased by increasing the sample length. Thus, the requirements on the excitation intensity can be reduced by considering longer sample with $L > 400\,\mu\text{m}$ to get significant parametric amplification and oscillation. These system specifications are also adequate in avoiding the possibility of any optical damage of the crystal. Experimentally, Ji et.al. [41] observed optical bistability in InSb crystal at excitation intensity of 1 MWcm^{-2} obtainable from 1.5 to 2 μs pulsed CO_2 lasers and did not notice any optical damage. The dependence of the power gain on the applied magnetic field is displayed in Fig. 3.

The curve manifests remarkable enhancement of the power gain only when a large magnetic field yielding $\omega_c \sim \omega_0$ is applied. The variation in $g_i(L)$ with change in the sample length L and the pump intensity I_p are shown in Figs. 4 and 5, respectively. These figures are plotted for $\omega_c = \omega_0$. It can be observed that $g_i(L)$ increases almost exponentially with increase in L as well as I_p. A similar observation of an intensity dependent power gain was reported by Rabson et.al. [42] in $Ba_2NaNb_5O_{15}$ single crystal where the idler was also an electromagnetic wave.

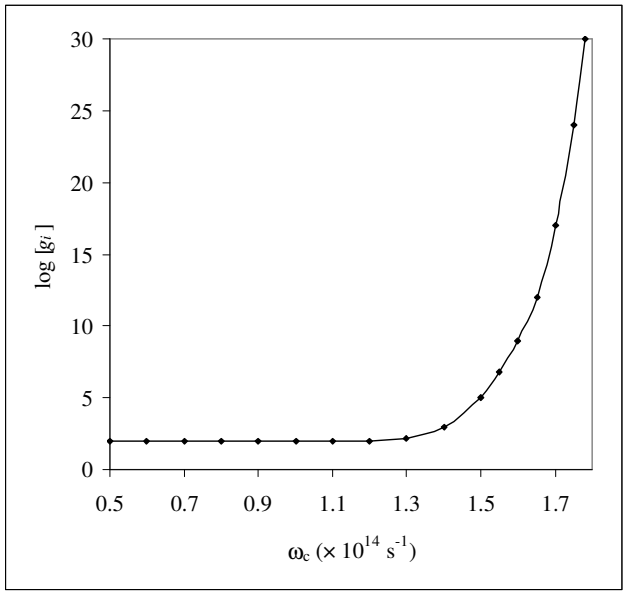

Figure 3: Variation of single-pass power gain $g_i(L)$ of the optical phonon wave with magnetic field B_s (in terms of ω_c). Here $n_0 = 2\times10^{21}\,\mathrm{m}^{-3}$ ($\omega_p = 5.4\times10^{12}\,\mathrm{s}^{-1}$) and $I_p = 10^{11}\,\mathrm{Wm}^{-2}$.

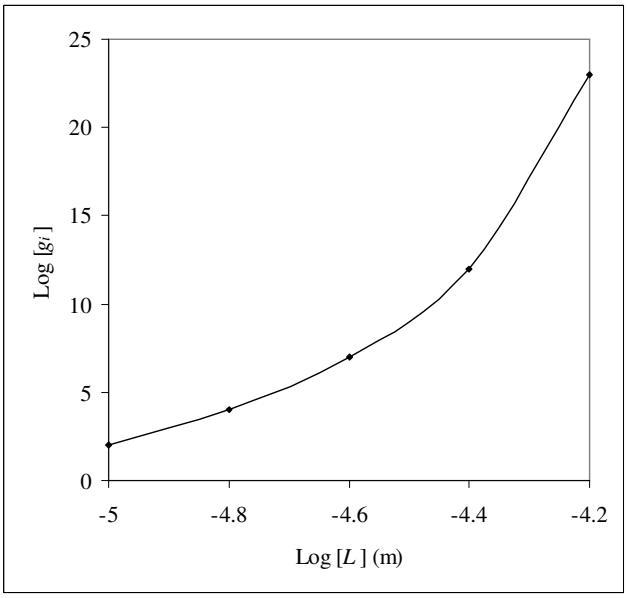

Figure 4: Variation of single pass power gain $g_i(L)$ with the sample length L. Here $B_s = 14.2\mathrm{T}$ ($\omega_c = 1.78\times10^{14}\,\mathrm{s}^{-1}$), $n_0 = 2\times10^{21}\,\mathrm{m}^{-3}$ ($\omega_p = 5.4\times10^{12}\,\mathrm{s}^{-1}$) and $I_p = 10^{11}\,\mathrm{Wm}^{-2}$.

We may expect from the above results and discussions that super-fluorescent parametric emission of the optical phonons can be observed in moderately doped III-V semiconductor crystals and subjecting it to a 10-nanosecond pulsed high power laser and a large magnetic field.

5.2 Threshold and conversion efficiency of SRPO

In this subsection, we examine the role of the magnetic field, on the threshold condition and the conversion efficiency of the SRPO using an n-InSb crystal.

We have fixed the doping level at $2\times10^{21}\,\mathrm{m}^{-3}$ (i.e. $\omega_p = 5.4\times10^{12}\,\mathrm{s}^{-1}$).

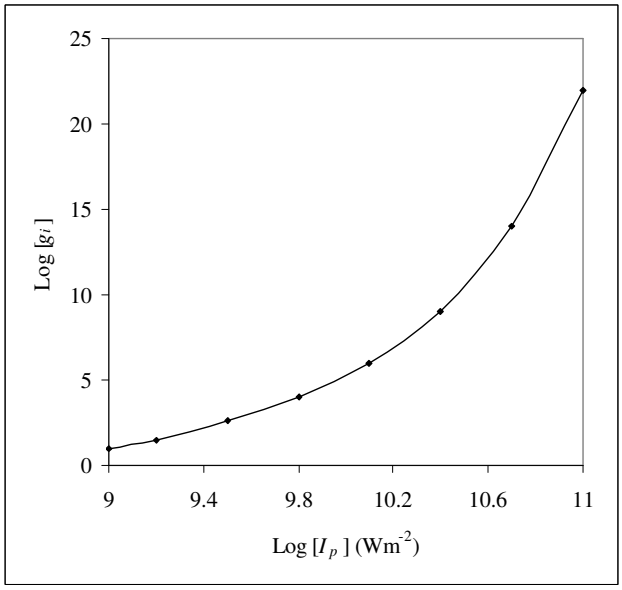

Figure 5: Variation of single pass power gain $g_i(L)$ with excitation intensity I_p well above the threshold. Here $L = 400\mu\mathrm{m}$, $B_s = 14.2\mathrm{T}$ ($\omega_c = 1.78\times10^{14}\,\mathrm{s}^{-1}$), $n_0 = 2\times10^{21}\,\mathrm{m}^{-3}$ ($\omega_p = 5.4\times10^{12}\,\mathrm{s}^{-1}$).

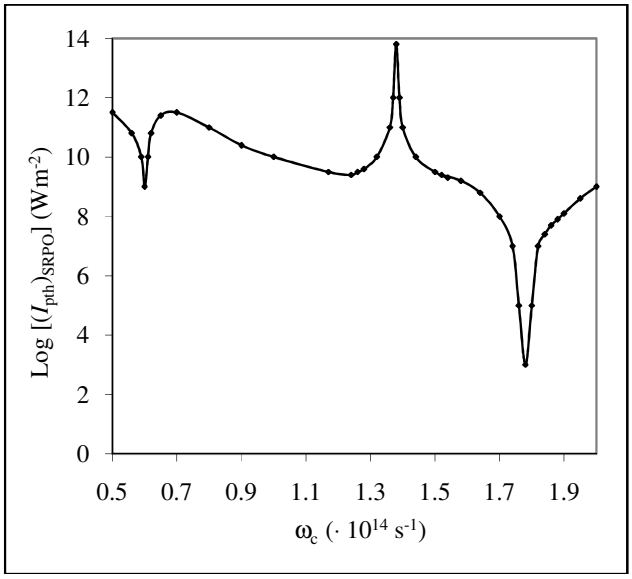

Figure 6: Variation of threshold intensity $(I_{pth})_{SRPO}$ of the single resonant parametric oscillator with the applied magnetic field B_s (in terms of ω_c). Here $n_0 = 2\times10^{21}\,\mathrm{m}^{-3}$ ($\omega_p = 5.4\times10^{12}\,\mathrm{s}^{-1}$).

Using Eq. (27), the qualitative behavior of the threshold intensity of SRPO $(I_{pth})_{SRPO}$ as a function of the magnetic field (in terms of ω_c) is plotted in Fig. 6 at fixed reflectivity $R_s = 95\%$ and sample length $L = 400\mu\mathrm{m}$. The qualitative nature of the variation of $(I_{pth})_{SRPO}$ is almost similar to that of $(I_{pth})_{PA}$ as shown in Fig. 1. Qualitatively, one can find that at low magnetic fields, $(I_{pth})_{SRPO}$ is so large that one may use semiconductors like n-InSb in SRPO when the crystal is subjected to a large magnetic field. Such a configuration can bring down the threshold intensity by about an order of 5 to 6. It has been also noticed that the $(I_{pth})_{SRPO}$ decreases sharply with the increase in the mirror reflectivity as well as sample length. These analytical results are in very good agreement with the experimental observations [43, 44].

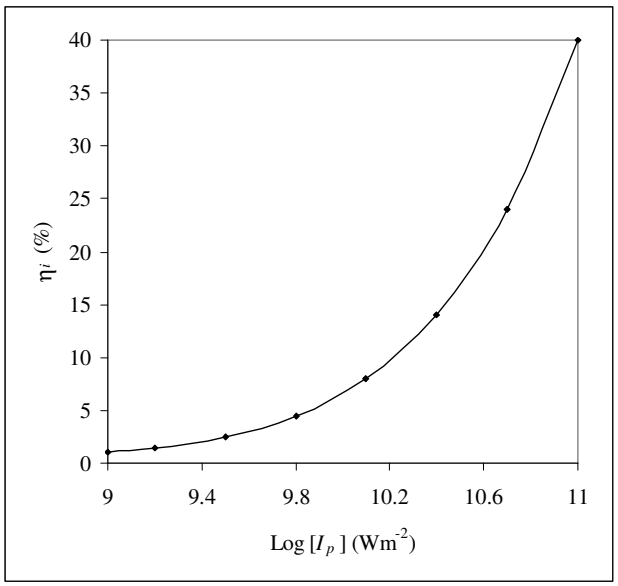

Figure 7: Variation of conversion efficiency η_i of the parametric oscillator with excitation intensity I_p. Here $R_s = 95\%$ and $L = 400\mu m$.

It is evident from Fig. 7 that if the crystal is subjected to a large magnetic field $B_s = 14.2\,T$ ($\omega_c \sim \omega_0$), and the excitation intensity I_p is well above the threshold, the conversion efficiency undergoes an almost exponential increase with rise in I_p. This is also compatible with the available experimental results but one may note in this connection that the excitation intensity cannot be increased arbitrarily and one should restrict to values of I_p well below the optical damage limit. Of course, the damage threshold can be raised by reducing the pump pulse duration and increasing the sample length.

4. Conclusions

The present article deals with the analytical investigation of the OPA and SRPO in a weakly polar semiconductor subjected to a large magnetic field. The numerical analysis is made for a 400 μm long n-InSb sample. The result suggests that efficient OPA/SRPO can be devised using III-V semiconductor crystal considering optical phonon scattering mechanisms.

Based upon optical phonon scattering mechanisms, the second-order optical susceptibility $\sim 1.6\times10^{-7}$ SI units in the presence of a magnetic field around 14.2 T. The application of a large magnetic field significantly reduces the threshold value of the pump intensity for the onset of parametric amplification and oscillation. At sufficiently high magnetic fields (i.e. $\omega_c \sim \omega_0$), the power gain is enhanced by a few orders of magnitude.

The conversion efficiency of SRPO is also enhanced significantly in the above resonant regime. The present numerical analysis indicates towards the strong possibility of achieving super-fluorescent parametric amplification in the infrared region under the consideration of

(i) a slightly off-resonant laser excitation with excitation intensity around 10 MWcm^{-2}; and

(ii) the optical phonon electric field much larger than the Stoke's field at the entrance window.

Acknowledgements

The author is very thankful to Dr. Manjeet Singh, Assistant Professor, Department of Physics, Government College, Matanhail, Jhajjar – 124106 (Haryana) India for many useful suggestions to carry out this research work and careful reading of the manuscript.

References

[1] A. Ashkin, Acceleration and traping of particles by radiation pressure, *Phys. Rev. Lett.* **24** (1970) 156-159.

[2] J. Homola, Present and future of surface plasmon resonance biosensors, *Anal. Bioanal. Chem.* **377** (2003) 528-539.

[3] A. Szoke, V. Danean, J. Goldhar, N.A. Kurnit, Bistable optical element and its applications, *Appl. Phys. Lett.* **15** (1969) 376-379.

[4] W.H. Louisell, *Coupled and Parametric Electronics*, Wiley, New York (1960).

[5] J.A. Giordmaine, R.C. Miller, Tunable coherent parametric oscillation in $LiNbO_3$ at optical frequencies, *Phys. Rev. Lett.* **14** (1965) 973-976.

[6] S.E. Harris, Proposed backward wave oscillation in the infrared, *Appl. Phys. Lett.* **9** (1966) 114-116.

[7] K.H. Yang, P.L. Richards. Y.R. Shen, Generation of far-infrared radiation by picosecond light pulses in $LiNbO_3$, *Appl. Phys. Lett.* **19** (1971) 320-323.

[8] D.S Chemla, E. Batifol, R.L. Byer. R.L. Herbst, Optical backward mixing in sodium nitrated, *Opt. Comm.* **11** (1974) 57-61.

[9] S.E. Harris, Tunable optical parametric oscillators, *Proc. IEEE* **57** (1969) 2096-2113.

[10] G.K. Samanta, M. Ebrahim-Zadeh, Continuous wave singly-resonant optical parametric oscillator with resonant wave coupling, *Opt. Express* **16** (2008) 6883-6888.

[11] S. Zou, M. Gong, Q. Liu, P. Yan, G. Chen, Gain width and rise time studies of pulsed unstable optical parametric oscillators, *Appl. Phys. B* **81** (2005) 1101-1106.

[12] A.I. Vodchits, V.I. Dashkevich, N.S. Kazak, V.K. Pavlenko, V.I. Pokryshkin, I.P. Petrovich, V.V. Rukhovets, A.S. Kraskovskii, V.A. Orlovich, Eye safe radiation source based on an optical parametric oscillator, *J Appl. Spectrosc.* **73** (2006) 285-291.

[13] O.B. Jensen, M. Brunn-Larsen, O. Balle-Petersen, T. Skettrup, Yellow nanosecond sum-frequency generating optical parametric oscillator using periodically poled $LiNbO_3$, *Appl. Phys. B* **91** (2008) 61-63.

[14] B. Ruffing, A. Nebel, R. Wallenstein, High power picosecond LiB_3O_5 optical parametric oscillators tunable in the blue spectral range, *Appl. Phys. B* **72** (2001) 137-149.

[15] P.A. Wolff, *Nonlinear Optics*, Academic Press, London (1977), pp. 169-211.

[16] R.L. Byer, *Quantum Electronics*, Academic Press, New York (1975), pp. 9-207.

[17] M. Singh, P. Aghamkar, S. Duhan, Enhancement of second- and third-order nonlinear optical susceptibilities in magnetized semiconductors, *Chin Phys. Lett.* **25** (2008) 3276-3279.

[18] A. Miller, D.A.B. Miller, S.D. Smith, Dynamic nonlinear optical processes in semiconductors, *Adv. Phys.* **30** (1981) 697-800.

[19] M.J. Rosker, C.L. Tang, Widely tunable optical parametric oscillator using urea, *J Opt. Soc. Am. B* **2** (1985) 691-696.

[20] F. Sanchez, P.H. Kayoun, J.P. Huignard, Two-wave mixing with gain in liquid crystals at 10.6 μm wavelength, *J Appl. Phys.* **64** (1988) 26-31.

[21] J.T. Lin, J.L. Montgomery, Generation of tunable mid-IR

laser from optical parametric oscillation in KTP, *Opt. Commun.* **75** (1990) 315-320.
[22] J. Takahashi, Parametric amplification of Raman-inactive lattice oscillations induced by two-color crossed-beam excitation, *Opt. Exp.* **14** (2006) 2831-2838.
[23] S. Dubey, S. Ghosh, Parametric oscillations of polaron modes in magnetized semiconductor-plasmas, *New J. Phys.* **11** (2009) 093030-093043.
[24] R.J. Elliott, A.F. Gibson, *An Introduction to Solid State Physics and its Applications*, McMillan, London (1974), p. 302.
[25] M. Cardona, *Light Scattering in Solids,* Springer Verlag, Berlin (1983), p. 11.
[26] S.S. Mitra, N.E. Massa, *Handbook on Semiconductors*, North- Holland, The Netherland (1982), pp. 83-189.
[27] W. Jones, N.M. March, *Theoretical Solid State Physics*, Dover, New York (1985), p. 613.
[28] M. Singh, Dependence on geometry of coherent Raman-scattered Stoke's mode in weakly polar magnetized semiconductors, *Physica B* **403** (2008) 3985-3989.
[29] K. Nishikawa, Parametric excitation of coupled waves. I. General Formulation, *J. Phys. Soc. Jpn.* **24** (1988) 916-922; Parametric excitation of coupled waves. II. Parametric plasmon-photon interactions, *J. Phys. Soc. Jpn.* 24 (1988) 1152-1158.
[30] J. Callaway, *Quantum Theory of the Solid State*, Academic Press, New York (1974), p.16.
[31] K. Seeger, *Semiconductor Physics*, Springer Verlag, Berlin (1989), p. 183.
[32] A. Yariv, P. Yeh, *Optical Waves in Crystals*, John Wiley, New York, (1984), p.319.
[33] G.K. Celler, R. Bray, Effect of screening of piezoelectric phonon fields on absorbing edge broadening in GaAs, *Phys. Rev. Lett.* **37** (1976) 1422-1425.
[34] P. Aghamkar, P.K. Sen, Parametric excitation of laser in magnetoactive doped piezoelectric semiconductors, *Phys. Status Solidi B* **157** (1990) 735-744.
[35] B. Ya Zel'dovich, N.F. Pillipetskii, V.V. Shkunov, *Principle of Phase Conjugation*, Springer-Verlag, Berlin (1985), p. 28.
[36] G. Bjork, Y. Yamamoto, Phase correlation in nondegenerate parametric oscillators and amplifiers: Theory and applications, *Phys. Rev. A* **37** (1988) 1991-2006.
[37] Y.R. Shen, *The Principle of Nonlinear Optics*, John Wiley, New York (1984), pp.117-140.
[38] M. Singh, S. Redhu, S. Duhan, R.S. Pandey, Steady-state and transient Raman gain in magnetoactive narrow-band gap semiconductors, *Opt. Laser Tech.* **42** (2010) 202-207.
[39] M. Singh, P. Aghamkar, S.K. Bhakar, Parametric dispersion and amplification in semiconductor-plasmas: effects of carrier heating, *Opt. Laser Tech.* **41** (2009) 64-69.
[40] P.K. Sen, Third-order susceptibility of III-V semiconductors in the true continuum near the band edge, *Solid State Commun.* **43** (1982) 141-146.
[41] W. Ji, A.K. Kar, U. Keller, J.G.H. Mathew, A.C. Walker, *Optical Bistability* III, Springer-Verlag, Berlin (1986), pp. 35-38.
[42] T.A. Rabson, H.J. Ruiz, P.L. Shah, F.K. Tittel, Stimulated parametric fluorescence induced by picosecond pump pulses, *Appl. Phys. Lett.* **21** (1972) 129-131.
[43] S.J. Brosnan, R.L. Byer, Optical parametric oscillator threshold and linewidth studies, *IEEE J. Quantum Electron.* **QE-15** (1979) 415-431.
[44] R.C. Eckardt, Y.X. Fan, R.L. Byer, C.L. Marquardt, M.E. Strom, L. Esterowitz, Broadly tunable infrared parametric oscillator using $AgGaSe_2$, *Appl. Phys. Lett.* **49** (1986) 608-610.